NURETH14-489

HEAT TRANSFER IN A NON ADIABATIC CALORIMETER: NUMERICAL PARAMETRIC STUDY WITHOUT AND WITH NUCLEAR HEATING DEPOSIT

O. MERROUN¹, C. REYNARD-CARETTE¹, A. LYOUSSI², J. BRUN¹, M. CARETTE¹, A. JANULYTE¹, Y. ZEREGA¹, J. ANDRÉ¹, G. BIGNAN², J-P. CHAUVIN², D. FOURMENTEL², C. GONNIER², P. GUIMBAL², J-Y.MALO², J-F. VILLARD²

Laboratoire Chimie Provence LCP UMR 6264 – University of Provence Centre St Jérôme, bât Madirel, 13397 Marseille cedex 20, France
Commissariat à l'Energie Atomique et aux Energies Alternatives, CEA², Direction de l'Energie Nucléaire
Centre de Cadarache, 13108 Saint-Paul-Lez-Durance, France christelle.carette@univ-provence.fr

Abstract

The numerical works presented in this paper belong to the IN-CORE (Instrumentation for Nuclear radiations and Calorimetry Online in REactor) research program. Its scientific aim is to create a new device dedicated to the online simultaneously measurements of nuclear conditions inside experimental channels of the Jules Horowitz Reactor (JHR) by coupling different sensors. This paper studies a specific one: a radiometric calorimeter used to in pile nuclear heating measurements. Numerical simulations on heat transfers taking place into this sensor under radioactive and non-radioactive conditions are carried out. The influence of the geometrical dimensions and of the energy deposit on the heat flux density, on the sensor sensitivity and on the maximum temperature is discussed.

Introduction

Inside a nuclear reactor core, the nuclear heating results mainly from the absorption and scattering of core neutrons and gammas with atoms of fuels and of structural materials. In fact, each interaction releases an amount of energy carried by the particles produced from these reactions and by gamma rays. The decay of unstable isotopes produced by the absorption reactions (n, γ) , (γ, n) , (n, α) , etc, contributes apparently to the total nuclear heating. Quantification of this phenomenon is of a great importance as it is in the center of interest of safety analysis concerning the temperature control of instrumentations housing the experimental irradiation channels. Nuclear heating can be measured by different methods: direct method such as calorimetry, gamma thermometer and indirect method such as ionization chambers [1]. Calorimeters is used as experimental devices for the quantitative measurement of nuclear heating in specific samples for engineering purposes of structural materials or for local measurements of nuclear heating [2-9].

At present, a real challenge concerns advanced online measurements of several parameters such as specific power deposit (W.g⁻¹), neutron and gamma flux inside experimental channels [10, 11]. Therefore, the great persisting challenge is to design new in pile instrumentations and measurement methods satisfying both safety requirements and scientific needs. The present works are performed into this scientific background. More precisely, these works belong to the IN-CORE

The 14th International Topical Meeting on Nuclear Reactor Thermalhydraulics, NURETH-14 Toronto, Ontario, Canada, September 25-30, 2011

(Instrumentation for Nuclear radiations and Calorimetry Online in REactor) research and development program which has been started in 2009 between the University of Provence (Marseille, France) and the CEA² (French Atomic Energy and Alternative Energies Commission) - Jules Horowitz Reactor (JHR) program. IN-CORE collaborative program belongs to the new CEA-Provence University join laboratory called LIMMEX. This European Material Testing Reactor (MTR) [11,12] will allow typically ~ 20 simultaneous experiences in the core and in the reflector. This MTR will provide, for researchers and end-users, experimental facilities with higher performances to carry out new experiments on structural material ageing and fuel behavior under irradiations. The results obtained will contribute for instance to the safety requirements or to the optimization of existing or coming nuclear power reactors as well as the developments of the future ones.

Two main subjects are developed in parallel in the IN-CORE program. The first one focuses on the development of an innovative technological device mixing different types of sensors as fission and ionization chambers for measuring neutron and photon fluxes, respectively, as well as a gamma thermometer and a radiometric calorimeter for quantifying nuclear heating [13]. The second one concerns a complementary analytical approach on a radiometric differential calorimeter focusing especially on heat transfer. This calorimeter has been developed previously by the CEA² and tested inside the OSIRIS reflector [14-16]. The aim of these analytical studies is to develop numerical and experimental tools [17, 18] to improve and/or to adapt the response of the calorimeter under several physical and geometrical conditions.

In first hand this is achieved by an analysis of heat transfer phenomena occurring inside the calorimeter and with its surroundings (cooling water) and in the second hand it is performed by interpreting the data sets resulting from in pile simulations.

This paper deals with presenting the numerical models developed for both irradiated and non irradiated conditions with a great interest for validation activities of the mathematical model describing the sensor calibration process. Simulation results concerning the response of the calorimeter are given. Practical interest in the effect of maximum power deposit (over the calorimeter structural material) and of the calorimeter dimension on the temperature, the heat flux fields, and the sensitivity is discussed.

1. Thermal analysis

1.1 Geometrical and operating mode of the sensor

The calorimeter corresponds to a differential calorimeter running in non-adiabatic mode or permanent mode. The calorimeter, shown schematically in Figure 1, corresponds to a simple robust design composed by two superposed twin cells contained in a cylindrical stainless steel tube filled with nitrogen gas. The upper cell includes a cylindrical head (containing an alumina tube with a resistance and a graphite sample acting as radiation absorber due to its elevated atomic density), a cylindrical aluminum base and a pedestal/rod which is placed between the head and the base. The lower cell does not contain graphite sample. It is replaced by an empty cavity filled with nitrogen gas. This lower cell is used as reference cell. Each cell is instrumented by means of two thermocouples. The first one is imbedded into the top of the pedestal and the second one into the base center allowing a differential measurement of temperature for each cell.

The 14th International Topical Meeting on Nuclear Reactor Thermalhydraulics, NURETH-14 Toronto, Ontario, Canada, September 25-30, 2011

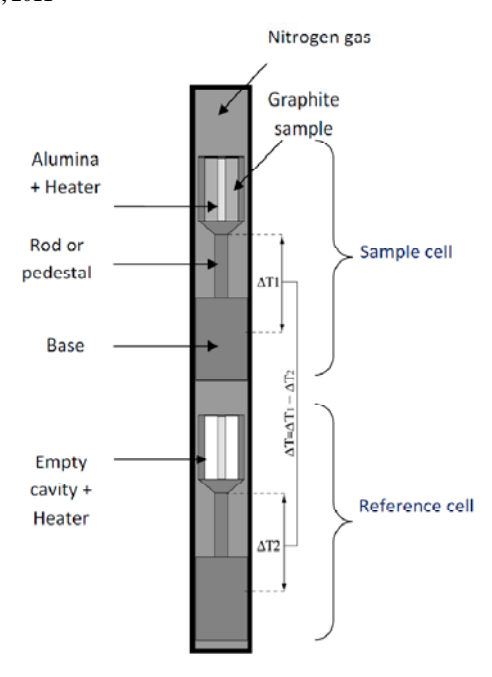


Figure 1 Differential calorimeter diagram

The operating mode used is a permanent mode with a heat flow (or heat exchange) between the calorimeter and its surroundings (water bath during calibration or water flow during irradiation). The heat generated in each cell, owing primarily to the absorption and scattering reactions of core neutrons and gammas with atoms in structural elements of the cells, is transferred through the base to the reactor coolant at the outside surface of the stainless steel cylindrical jacket. The nitrogen gas surrounding the cells is considered as a thermal isolation shield due to its low-conductivity limiting heat losses.

1.2 Heat transfer model

1.2.1 Mathematical model

Heat transfers inside the calorimeter occur mainly by the conduction mode in the structural elements of the calorimeter. The nitrogen gas inside the cells is considered as a static gas cavity described by heat conduction law.

Hereafter, the heat transfer model is described for two distinct cases.

The first one corresponds to the calorimeter calibration under non irradiated conditions. In that case the calorimeter is inserted in a water bath with a constant bulk temperature (Figure 2-a) without water flow. The nuclear heating is simulated by heating the graphite sample by Joule effect by means of a heater element inserted into the alumina. Then, the heat produced is diffused from the head towards the cell base through the pedestal/rod. The second model concerns heat transfers in an irradiated medium. In these conditions, and contrary to the calibration experiments where the electric power is injected only on the alumina heater, the calorimeter is exposed to nuclear radiation flux and its structural materials are entirely heated. This implies that the heat generated should be taken as a spatial distribution according to axial ordinate (the radial gradient of nuclear heating is

neglected). Figure 2-b schematizes the experiment done inside OSIRIS research reactor at CEA-Saclay.

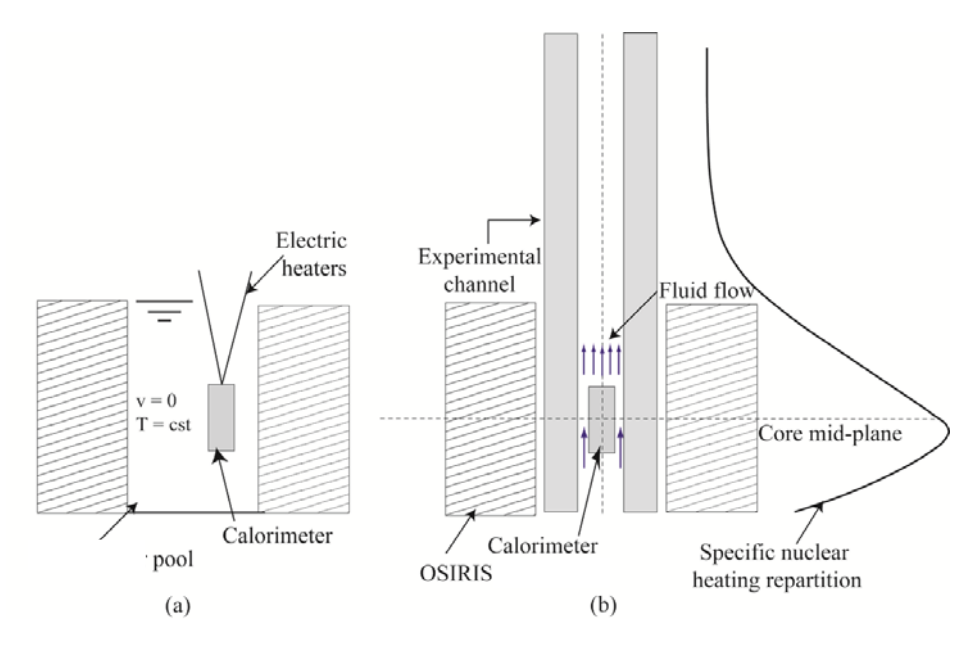


Figure 2 (a) Calibration experiment under non irradiated conditions; (b) The calorimeter inside an experimental channel under irradiated conditions

The mathematical model describing the heat transport inside the sensor is developed on the basis of the following assumptions:

- Computational domain is considered bi-dimensional due to the axi-symmetrical geometry of the twin cells
- Thermal expansion effects and the radiative exchanges are neglected. The thermal conductivity of materials is calculated based on the variable temperature.
- Bulk liquid temperature surrounding the calorimeter tube is equal to 23 °C during calibration and equal to 30°C inside the experimental channel of the reactor. Thermal properties of water are estimated at these temperatures.
- Heat fluxes evacuated through the lower and upper horizontal walls of the stainless steel tube are neglected.
- Heat dissipated in the calorimeter is evacuated through:
 - (i) Natural convection under non irradiated conditions,
 - (ii) Forced convection under irradiated conditions.
- Heat source term corresponds to the heat produced by:
 - (i) Joule effect inside the resistance for calibration experiments. This quantity is equal to zero everywhere in the calorimeter except in alumina containing the heater.
 - (ii) Neutrons/gammas interactions with atoms of the medium for irradiated experiments. The heat source depends in particular to the location of the device (core or reflector core), to the device altitude in the irradiated channels (only the axial gradient of the nuclear heating is taking into account), to its structural materials.

The heat flow across the graphite sample, the pedestal/rod, the base is determined by the following equation considering the isotropic and homogenous properties of materials:

The 14th International Topical Meeting on Nuclear Reactor Thermalhydraulics, NURETH-14 Toronto, Ontario, Canada, September 25-30, 2011

$$\rho_i C p_i \frac{\delta T}{\delta t} = \lambda_i \frac{1}{r} \frac{\delta}{\delta r} \left(r \frac{\delta T}{\delta r} \right) + \lambda_i \frac{\delta^2 T}{\delta z^2} + Q_i \tag{1}$$

where ρ_i is the mass density of a given material i [kg/m³], Cp_i is the heat capacity of a given material i [J/(Kg. K)]. λ_i is the thermal conductivity of material i [W/(m. K)], Q_i is the heat generation per unit of volume of a given material i [W/m³].

As we have previously reported for non-irradiated medium the source term Q_i , is null on all structural materials of the calorimeter except on the resistance tube where it is defined from Ohm's law. In irradiated environment, the specific nuclear heating in OSIRIS for a given material i of atomic number Z and at an altitude z of the core mid-plane can be defined as:

$$S_i(z,Z) = S_i(z=0,Z=6)F_i(Z)f(z)$$
 (2)

where S(z=0,Z=6) represents the specific nuclear heating within a graphite sample at the reactor core mid-plane (W/g), F(Z) is a factor depending rigorously of the results of core neutron/photon transport calculation, and f(z) is a characteristic curve representing the vertical repartition of the total nuclear heating along each experimental channel. Mathematically, the source term Q_i should be defined on each node of the calorimeter computational domain as power per unit of volume (W/m³). Consequently, for a given material of atomic number Z, the local thermal power is obtained by multiplying the specific nuclear heating function (S(z, Z)) by the atomic density of each material:

$$Q_i(z,Z) = S_i(z,Z)\rho_i \tag{3}$$

1.2.2 <u>Initial and boundary conditions:</u>

For time-dependent problems, an initial condition for the temperature field, i.e. $T(R, z; t_0) = T_o(R, z)$ at $t_0 = 0$ has to be specified as $T_0 = T_b$ where T_b is the bulk fluid temperature.

Concerning the boundary conditions of the problem, neither the temperature T nor the heat flux φ are known at the external surface of the stainless steel cylinder. In this case, the heat flux exchanged at the interface solid-liquid can be evaluated thanks to the convective heat transfer coefficient h.

This heat transfer coefficient can be evaluated by means of empirical correlations using the calculation

of the Nusselt number
$$\left(h = \frac{\lambda}{D} Nu\right)$$
. In particular it depends on the fluid flow regime around the tube.

In the case of the calibration tests (medium without radiations), the convective heat transfer corresponds to natural convective flows around a heated vertical cylinder at a constant heat flux. The average Nusselt number on the surface of vertical cylinder is given by the following correlation [19]:

$$Nu_{av} = 0.55 \left(Ra_D^* \frac{D}{L} \right)^{0.20}$$
 (for Ra_D D/L>10⁴) (4)

where Ra_D^* corresponds to the modified Rayleigh number calculated from the heat flux, L the tube length and D the tube diameter.

In an irradiated channel of OSIRIS, the cooling flow condition corresponds to turbulent forced convection. For fully developed fluid flow inside an annular domain (between the calorimeter and the experimental channel) and for all values of Prandtl number, the averaged Nusselt number used can be determined by the modified Colburn Correlation given by [20] and with the Reynolds number calculated from the hydraulic diameter.

The 14th International Topical Meeting on Nuclear Reactor Thermalhydraulics, NURETH-14 Toronto, Ontario, Canada, September 25-30, 2011

$$Nu_{av} = 0.023 \,\mathrm{Re}^{0.8} \,\mathrm{Pr}^{1/3} \left(\frac{d_{ext}}{d_{int}}\right)^{0.14}$$
 (5)

1.2.3 Numerical solution

The computational domain of the calorimeter is discretized using the finite element method. It is implemented by using the 2009 CAST3M code release, developed by the French Atomic Energy and Alternative Energies Commission (CEA²). It is a general purpose code to solve linear and non-linear partial differential equations by the finite element method. Figure 3 shows the computational domain meshed by two kinds of element: (i) three node triangular elements are used to mesh nitrogen gas cavities and the cone of the graphite sample holder (the lower section of cell head), and (ii) four nodes quadrilateral meshes for the remaining calorimeter structural elements.

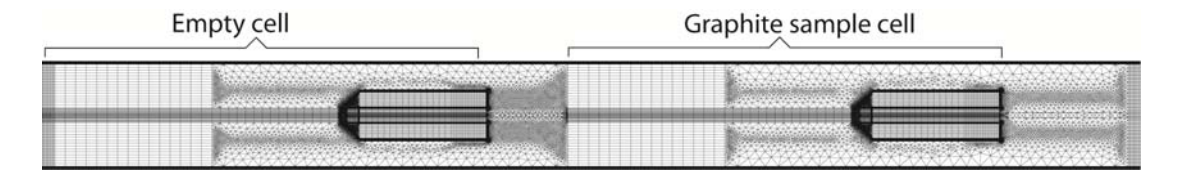


Figure 3 Computational domain discretization

The non-linear heat conduction equation is solved iteratively by using a procedure repeated until satisfying the following convergence criterion:

$$Res(T) = \rho_i C p_i \frac{\delta T}{\delta t} - \lambda_i \frac{1}{r} \frac{\delta}{\delta r} \left(r \frac{\delta T}{\delta r} \right) - \lambda_i \frac{\delta^2 T}{\delta z^2} - Q_i < \varepsilon$$
 (6)

where ε is a predefined tolerance (ε =10⁻⁶) and Res(T) is the residual vector.

2. Results and discussions

In nuclear engineering and design disciplines, numerical simulation tools are widely used by scientists and engineers to take crucial decisions according to the safety requirements. This implies that, before considering simulation codes as reliable predictive tools of a physical phenomenon, they have to be validated. Otherwise, simulation results should well-reproduce experimental responses. In projecting this concept into our study, we have proceeded, first of all, to corroborate the mathematical model implemented in CAST3M code which describes the heat transfer inside the calorimeter and with its surroundings under non irradiated conditions.

Even if, in the case of the calibration under non irradiated conditions, the absolute value of the temperatures does not correspond to those obtained in pile, this preliminary step is crucial in order to quantify the sensor sensitivity. In addition a validated numerical model under non irradiated conditions is interesting in order to determine the heat flux distribution, to choose the thermocouple locations, and consequently to improve the calorimeter thermal behaviour and thus to improve its sensitivity.

2.1 Non irradiated medium: calibration experiments and parametric study

2.1.1 Validation

The validation process presented thereafter is based on the comparison between the calorimeter responses obtained with CAST3M computational model and the experimental responses measured during the calibration of the calorimeter under non irradiated conditions, experiments performed by CEA².

These works aim to characterise the sensor response versus the electrical power (sensitivity, temperatures, response time, and linearity). In practice, these calibration tests have been established through the injection of an electric current (corresponding to a power range going from 0.017 to 4.3 W) within each resistance inserted in the alumina tube.

Figure.1 shows the four thermocouple locations for the sample cell and the empty one. The simulation results are presented in Table 1 for 13 power levels.

Power (W)		Simulation (°C)				Relative error %			
Empty cell	Graphite cell	$T1_{rod}$	T1 _{base}	$T2_{rod}$	T2 _{base}	$T1_{rod}$	T _{base}	T2 _{rod}	T2 _{base}
4.3068	4.0958	78.6	27.2	75.3	26.6	2.92	6.61	2.52	3.75
3.5594	3.3849	69.2	26.6	66.5	26.1	3.46	6.01	2.70	3.44
2.6150	2.4869	57.2	25.8	55.1	25.4	3.14	3.87	2.90	2.36
1.8160	1.7270	46.9	25.1	45.5	24.7	2.98	2.39	2.63	2.42
1.4710	1.3989	42.4	24.7	41.3	24.5	3.06	2.42	2.42	1.22
1.1622	1.1053	38.4	24.4	37.5	24.2	3.64	2.86	2.66	1.65
0.8898	0.8462	34.8	24.1	34.1	23.9	3.16	2.07	2.34	1.67
0.6538	0.6217	31.7	23.9	31.2	23.7	2.83	1.25	1.92	1.26
0.4540	0.4318	29.1	23.6	28.7	23.5	2.06	1.69	1.74	0.85
0.2906	0.2763	26.9	23.4	26.7	23.3	1.85	1.28	1.12	0.85
0.1634	0.1554	25.2	23.2	25.1	23.2	1.19	1.29	0.39	0.43
7.26E-02	6.91E-02	24.0	23.1	23.9	23.1	0.83	0.86	0.41	0.00
1.82E-02	1.73E-02	23.2	23.0	23.2	23.0	0.86	0.86	0.43	0.00

Table 1 Comparison between the measured temperatures and the predicted ones obtained by CAST3M code for different power levels.

The analysis of the results shows that the numerical results fairly match with the experimental measurements with some discrepancies observed. They are always lower than the experimental ones and the discrepancies depend primarily on the power level injected within the resistance. The highest discrepancies are observed for the base temperatures and for the maximal power levels. For instance, for the rod temperature, this relative error doesn't exceed 4%. The behaviour difference can be due in particular to the boundary conditions imposed in the thermal model such as the adiabatic conditions imposed on the horizontal walls of the stainless steel tube or the correlation chosen (5) or a neglected thermal contact resistance between the base and the external stainless steel jacket. This behaviour difference will be studied.

For each operating conditions, the response of the sample cell is determined by calculating the temperature difference between $T1_{rod}$ and $T1_{base}$ in order to define the calibration curve. In Figure 4, the numerical calibration curve of the sample cell is given for an electric power lower than 5W. We observe that, the temperature difference varies linearly with the electric power injected in the resistance inserted into the alumina.

The numerical temperature difference is always overestimated but discrepancies between simulations and experimental results are always lower to 5%.

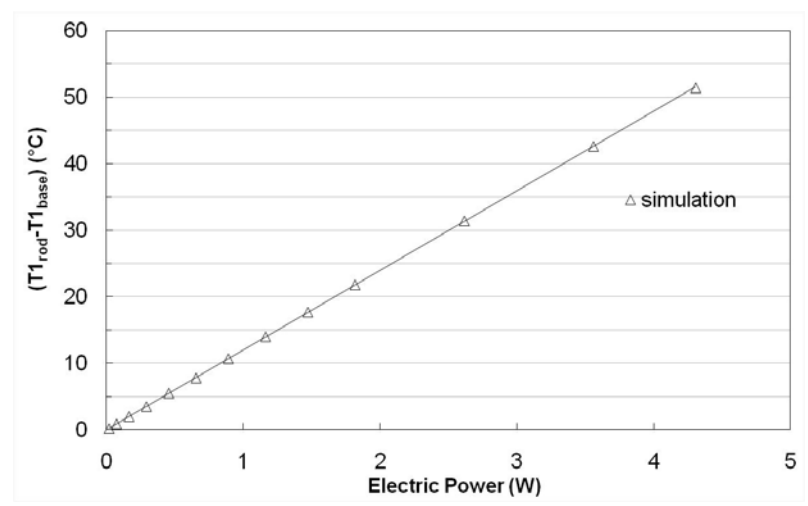


Figure 4 Calibration process of the graphite cell: T1_{rod}-T1_{base} versus the electric power

From the slopes calculated for each cell, the sensitivity of the calorimeter is determined. The aim of the numerical works is to study the influence of various parameters on the sensor response in order to improve the sensitivity according to the energy deposit range.

2.1.2 <u>Heat flux density</u>

On the one hand, the numerical results are analyzed in order to obtain the local radial heat flux density through the external tube. A wide range of electric powers imposed on the sample cell has been simulated (higher values than the experimental operating conditions).

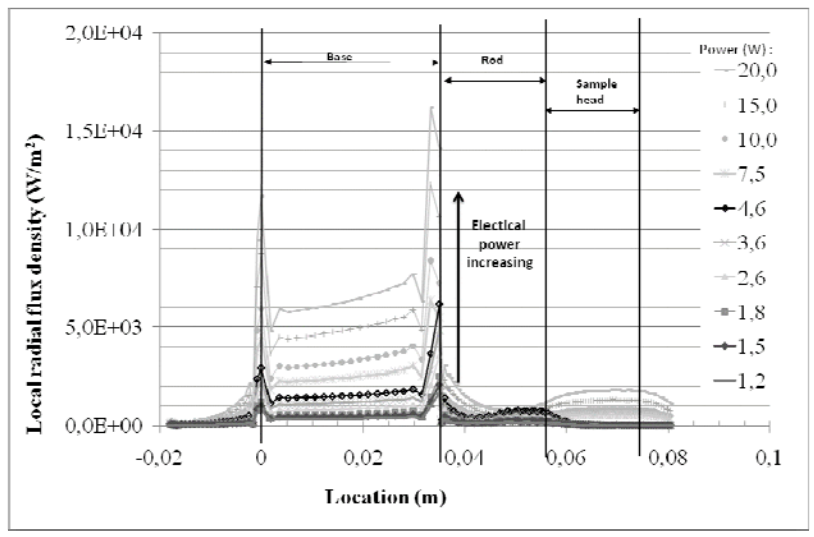


Figure 5 Local radial flux density along the external surface of the stainless steel jacket for various electric powers

The Figure 5 represents the local radial heat flux density versus the vertical ordinate of the stainless tube. A significant increase is observed at the base level.

On the second hand, the radial heat flux density is integrated on five areas along the external jacket corresponding respectively to the base level, the rod level, the sample cell head, the upper and the lower levels of the sample cell corresponding to the gas cavities.

The Figure 6 gives the relative repartition between the dissipated electric power in each areas and the electric power injected inside the sample head. These curves show that the calorimeter design ensures a good heat flow in the vertical direction because more than 70% of the electric power are evacuated through the base level surface. ~10% of the energy are exchanged at the level of the sample cell head. The thermal radial resistance of cylindrical gas layer around the sample head could be increased in order to decrease the heat losses and consequently to improve the axial heat flow.

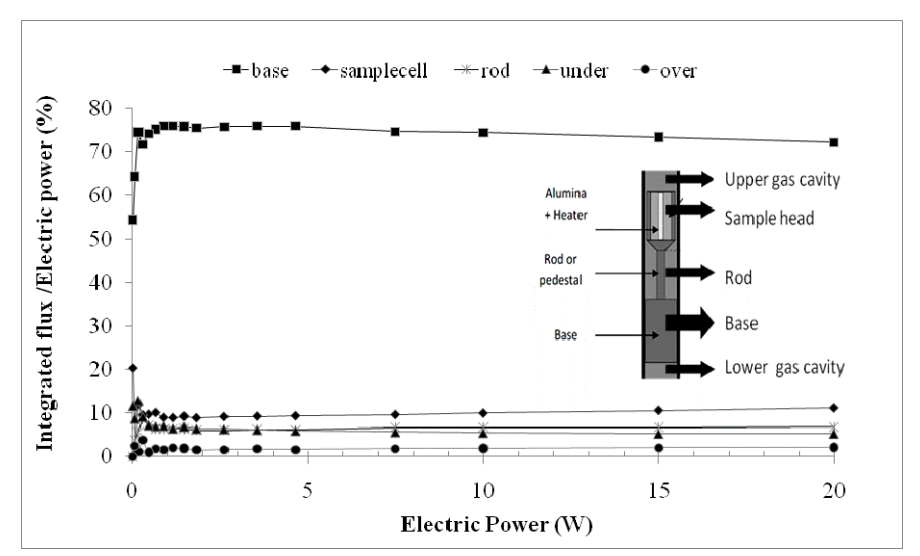


Figure 6 Distribution of the electric power dissipated by the sample cell along the external jacket

2.1.3 Sensitivity

The sensitivity of the sensor is also investigated versus some geometrical parameters of the calorimeter such as the rod or the base length, the rod radius. For each simulated dimension, the sensor response is determined.

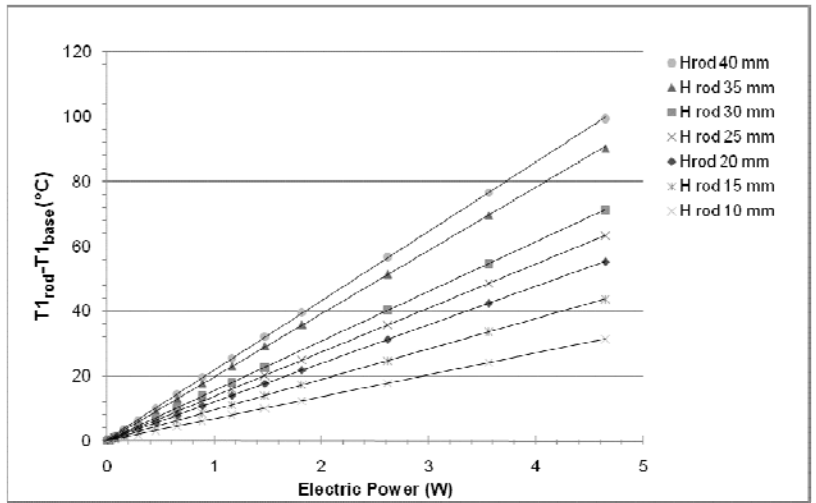


Figure 7 Temperature difference (T1_{rod}-T1_{base}) of the sample cell versus the electric power for different rod lengths

Figure 7 shows the influence of the rod length on the temperature difference of the sample cell. We note that for each geometrical dimension used, the sample cell response versus the electric power is linear for values lower than 5W. An increasing of the rod length (corresponding to a thermal resistance increasing) leads to the increasing of the temperature difference and consequently to the sensitivity of the calorimeter.

However in the case of designing an in pile device coupling instrumentations with the calorimeter, the available space is very crucial. Consequently, the increasing of the rod length has to be done simultaneously with a decreasing of the base length. The study of the sensitivity versus the base length and the rod radius has been carried out. The numerical results are summarized on the figure 8. This study confirms that the base length has no influence on the sensitivity, thus the variation of the rod length is possible. In addition, the influence of the rod radius is significant but the sensitivity does not depend on the square radius (a factor of 1.5 instead of 2 given by the regression). This behavior can be due to the thermocouple location and to the heat losses through the external jacket.

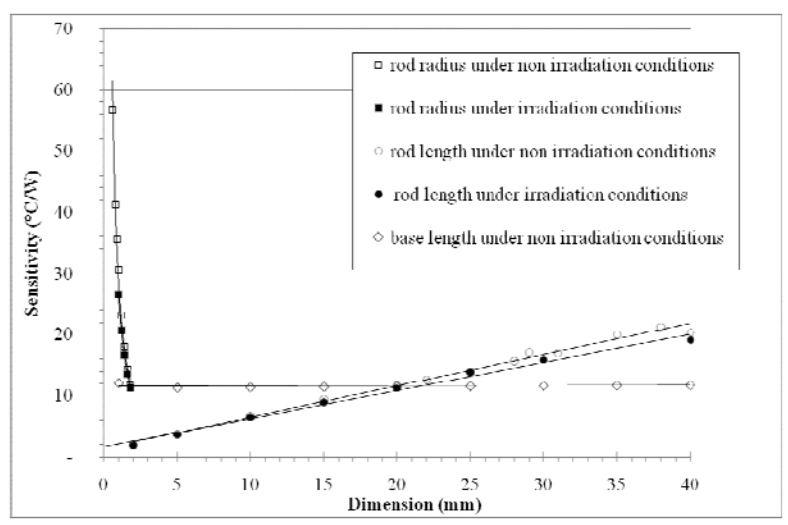


Figure 8 Calorimeter sensitivity versus the rod length, the rod radius and the base length: under non irradiated conditions (empty marks) and under irradiated conditions (filled marks)

2.2 Irradiated conditions

During experiments under irradiated conditions, the calorimeter is moved into the experimental channel in order to avoid the axial nuclear heating gradient and to obtain the temperature differences of the two cells for the same nuclear heating. Consequently, the numerical results are determined from two successive calorimeter locations.

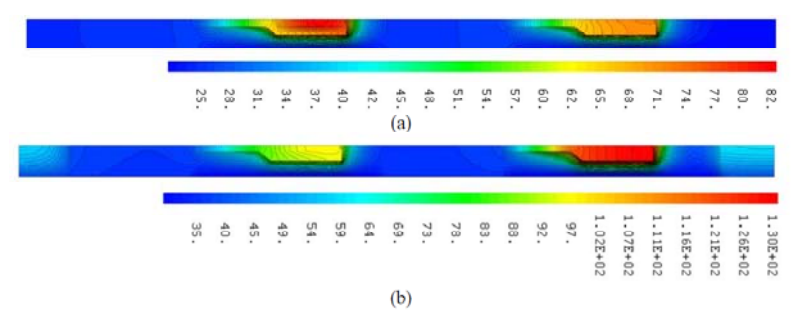


Figure 9 Temperature field of the calorimeter (2W/g): (a) Non-irradiated conditions and (b) Irradiated conditions

On the one hand, on Figure 8 we can see that the sensitivity does not depend on the conditions (under irradiated conditions: filled symbols, under non irradiated conditions: empty symbols). The calorimeter response is quite similar for the two cases. Thus with the operating principle based on a double temperature difference between the two twin cells (cf. Figure 1), the influence of the nuclear heat deposit on the calorimeter structure and on the stainless tube under irradiated conditions is withdrawn and the double temperature difference measured corresponds directly to the heating deposit into the graphite sample.

450 Conf3: Rrod = 2/3 Rrod conf2, 11rod=11rod conf2 400 Conf 2: Hrod 2Hrod conf1, Rrod Rrod conf1 350 300 Imax (°C) 200 150 100 50 3,0 1.5 2.0 3.5 W/g

Figure 10 The maximum temperature inside the calorimeter versus the nuclear heat deposit for three configurations

On the second hand, this model allows to predict the absolute temperature field under irradiated conditions. It is necessary to confirm that new designs respect temperature safety conditions. The Figure 9 represents an example of the temperature field inside the calorimeter for a heat deposit equal to 2 W/g. In the case (a), the same electric power is injected inside the sample cell and inside the reference cell which reaches a higher temperature due to a higher thermal isolation without the graphite. In the case (b), the axial gradient of the nuclear heating is taking into account.

In spite of the forced convection (velocity: 1m/s), the maximum temperature in the sample cell is around 130°C under irradiated conditions whereas it is equal to 70°C under non irradiated conditions.

Configuration	Rod Radius (Rrod)	Rod Height (Hrod)
Conf1	1.8 mm	20 mm
Conf2	1.8mm	40 mm
Conf3	1.2 mm	40 mm

Table 2: Dimensions of the calorimeter associated to three configurations

The last Figure 10 illustrates the influence of the dimension on the maximum temperature inside the calorimeter for three configurations (Table 2). When the rod length is doubled (conf2), the maximum temperature increases of 96 °C, and when the rod radius is multiplied by 2/3 (conf3) by keeping the doubled rod length, the maximum temperature increases still of 122 °C.

3. Conclusion and Outlooks

The analytical validated numerical works under non irradiated conditions (corresponding to calibration experiments) detail the thermal behavior of the calorimeter for various electric powers. Even if the

calorimeter design allows a good axial heat flow (70 % of the electric power are evacuated through the base), an optimization will be studied in order to decrease the radial heat exchange above the base. The response curve of this sensor is linear for the tested electric power range and for the different dimensions (<5W). The comparison between the sensitivity obtained with the calibration model under non irradiated conditions and with the model under irradiated conditions shows a good agreement. The model under irradiated conditions can be used to estimate the maximum temperature.

On the one hand these works will be completed in order to evaluate the uncertainties induced by various factors such as the mesh resolution, the heat transfer coefficient and the material properties. On the second hand other parametric studies will be performed in order to define a miniaturized calorimeter and to reach a specific calorimeter configuration dedicated to the experimental channels in the reactor core.

Acknowledgements

The IN-CORE program is supported by FEDER and Conseil Régional PACA.

References

- [1] In core Instrumentation for Online nuclear heating Measurements of Material Testing Reactor, C. Reynard et al., RRFM Transactions 2010, Marrakech, Morocco.
- [2] Differential calorimeter based on the heat leak principle, Biltonen et al. March 1981, US Patent References: 4255961.
- [3] Radiometric calorimetry: A review, Gunn, S. (1964), Nuclear Instruments and Methods 29(1), 1 24.
- [4] Radiometric calorimetry: A review (1970 supplement), Gunn, S. (1970), Nuclear Instruments and Methods 85(2), 285 312.
- [5] Radiometric calorimetry: A review: 1976 supplement', Gunn, S. (1976), Nuclear Instruments and Methods 135(2), 251 265.
- [6] Measurements of Nuclear Heating Rate and Neutron Flux in HANARO CN Hole for Designing the Moderator Cell of Cold Neutron Source, M-S. Kim, S-Y. Hwang, H-S.Jung and K-H. Lee, Proceedings of IGORR 2005
- [7] Benchmark of heat deposition measurement techniques in the SAFARI-1 reactor using MCNP5, B.M Makgopa, M. Belal, RRFM Transactions 2009.
- [8] Simulation of the In-Core Calorimeter Experiment in the SAFARI-1 Reactor, B.M Makgopa, M. Belal, ANIMMA International Conference, 7-10 June 2009, Marseille, France
- [9] IN-CORE Nuclear heating rates easily measured with proven calorimetric instruments, E.J. Allen, H. T. Kerr, J.F. Minecy, ORNL, Tennessee 37830, ANS Annual meeting, June 12-16, 1977, New York [10] Innovative in-pile instrumentation developments for irradiation experiments in MTRs, J-F. Villard, IGORR 2005.
- [11] Developments status of irradiation devices for the Jules Horowitz Reactor, C. Gonnier, D. Parrat, S. Gaillot, J.P. Chauvin, F. Serre, G. Laffont, A. Guigon, P. Roux, Research Reactor Fuel Management (RRFM) Transactions 2008.
- [12] Materials subjected to fast neutron irradiation, Jules Horowitz Reactor: a high performance material testing reactor, D. Iracane, P. Chaix, A. Alamo, C. R. Physique Vol. 9, 2008, pp. 445–456.
- [13] Combined analysis of neutron and photon flux measurements for the Jules Horowitz Reactor core mapping, D. Fourmentel, J-F. Villard, A. Lyoussi, C. Reynard-Carette, G. Bignan, J-P. Chauvin, C. Gonnier, P. Guimbal, J-Y. Malo, M. Carette, A. Janulyte, O. Merroun, J. Brun, Y. Zerega and J. André, , 2nd International Conference ANIMMA, June 2011, Ghent (Belgium)
- [14] H.Carcreff, Patent N° FR 1060068, December 3, 2010.

The 14th International Topical Meeting on Nuclear Reactor Thermalhydraulics, NURETH-14 Toronto, Ontario, Canada, September 25-30, 2011

- [15] CALMOS: Innovative Device for the Measurement of Nuclear Heating in Material Testing Reactors, H.Carcreff, ISRD14, 22-27 May 2011.
- [16] Development, calibration and experimental results obtained with an innovative mobile calorimeter (CALMOS) for nuclear heating measurements, H.Carcreff, V.Clouté-Cazalaa, L.Salmon, 2nd International Conference ANIMMA, June 2011, Ghent (Belgium).
- [17] Numerical study of heat transfer in radiometric calorimeter dedicated to nuclear heating measurements, C. Reynard-Carette, O. Merroun, J. Brun, M. Carette, A. Janulyte, Y. Zerega, J. André, P. Di Rosa, A. Lyoussi, G. Bignan, J-P. Chauvin, D. Fourmentel, C. Gonnier, P. Guimbal, J.Y.Malo, J-F. Villard, RRFM 2011, Rome, Italy, 20-24 March 2011.
- [18] Numerical and Experimental Calibration of Calorimetric Sample Cell Dedicated to Nuclear Heating Measurements, J. Brun, C. Reynard, O. Merroun, A. Lyoussi, M. Carette, A. Janulyte, Y. Zerega, J. Andre, G. Bignan, J-P. Chauvin, D. Fourmentel, C. Gonnier, P. Guimbal, J-Y. Malo and J-F. Villard, 2nd International Conference ANIMMA, June 2011, Ghent (Belgium).
- [19] Free-Convective Heat Transfer, Oleg G. Martynenko Pavel P. Khramtsov, Springer, 2005.
- [20] Transferts thermiques, Jean Taine, Estelle Iacona, Jean-Pierre Petit, Dunod, 2008.